

An Analysis of a Double-layer Electromagnetic Shield for a Universal Contactless Battery Charging Platform

X. Liu and S.Y.R.Hui, *Fellow IEEE*
Department of Electronic Engineering
City University of Hong Kong
Tat Chee Avenue, Kowloon
Hong Kong, China
(email: eeronhui@cityu.edu.hk)

Abstract—A patented double-layer planar structure is employed to shield the electromagnetic (EM) field at the bottom of a universal charging platform. The double-layer consists of a layer of soft ferromagnetic material and a layer of conductive material. Thin 4F1 ferrite plate and the copper sheet are used in this example. This shielding technique is analyzed with the extended transmission line theory. With the formulas presented, the shielding effectiveness (SE) of both single-layer shield and double-layer shield could be calculated out directly, without using finite-element software. A classical transmitting-receiving loop measurement has been carried out to evaluate the SE of single ferrite shield, single copper shield and double-layer shield respectively. Calculated and measured results in the working frequency range of the charging platform from 100 kHz to 500 kHz confirm that the double-layer shield has obviously better SE than single-layer shield and can achieve a SE above 40dB, which is commonly accepted by the industry. Finally, the potential of this double-layer shielding technique for a wide range of power electronic applications is discussed.

I. INTRODUCTION

A new generation of planar inductive battery charger for portable consumer electronic equipment as shown in Fig.1 has been presented in [1,12-14]. Different types of portable electronic equipment can be placed and charged simultaneously on the charging platform, regardless of their positions and orientations. An important design issue of the charging platform is the electromagnetic (EM) shield at the bottom of the platform. If EM field is not shielded in the bottom of the platform, undesirable energy transfer will take place when the charging platform is placed on a metallic table. To achieve a good shielding effectiveness (SE), a patented double-layer shield [2,10] has been employed. In [2,10], the shielding technique is analyzed from the magnetic field theory, and the shielding effectiveness is calculated

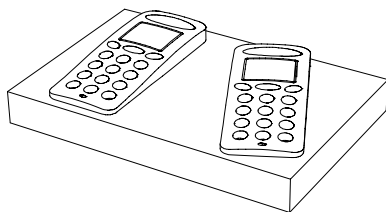


Fig. 1: Concept of a universal planar charging platform [1,12-14]

from the simulation results by finite element (FE) software. In this paper, the SE of this shielding technique is analyzed with the extended transmission line theory [3][4]. With the formulas presented, the SE of single-layer and double-layer shield could be calculated directly, without the use of the FE method. Some measurements are carried out from the frequency of 10 kHz to a few mega-Hertz to verify the calculation method. Measured results of the double-layer EM shield show a good shielding property in the working frequency range of the charging platform from 100 kHz to 500 kHz. The proposed double-layer EM shield structure can be constructed with flexible soft magnetic materials and conductive materials if necessary. This flexibility enables the proposed EM shield to be applied to a wide range of applications.

II. STRUCTURE OF THE CHARGING PLATFORM WITH THE DOUBLE-LAYER SHIELD

The cross-sectional structure of the charging platform with the double-layer shield is shown in Fig.2. The charging platform consists of three layers of hexagonal windings, which can generate magnetic flux of almost uniform magnitude over the surface of the winding arrays. The platform is driven by a power inverter as shown in Fig.3, working at a frequency chosen within the range from 100 kHz to 500 kHz, which is controlled by a standard PWM control IC. The double-layer shield is placed below the platform with an insulating layer inserted between them. In this example, the ferrite plates are made of 4F1 ferrite material [5]. The relative permeability, μ_r , and resistivity, ρ , of the 4F1 ferrite material are about 80 and $10^5 \Omega\text{m}$, respectively. The copper plates are adhibited directly under the ferrite plates. The thickness of the ferrite and the copper plates are 0.4 mm and 70 μm respectively.

III. SHIELDING EFFECTIVENESS ANALYSIS WITH THE EXTENSION OF TRANSMISSION LINE THEORY

Shielding effectiveness is defined as the ratio between the field strength, at a given distance from the source, without the shield interposed and the field strength with the shield interposed [6]. The manner in which an electromagnetic shield transmits electromagnetic waves has been shown to be analogous to the manner in which a conventional two-wire transmission line transmits electrical current and voltage [3][4]. With reference to Fig.4, comparison of the electromagnetic shield and the transmission line is listed in Table 1.

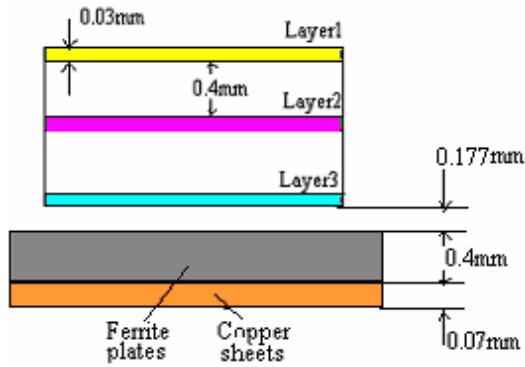


Fig. 2: The cross-sectional structure of the platform with double-layer shield

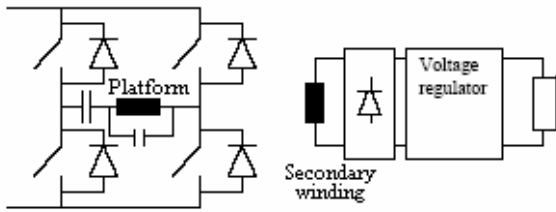


Fig. 3: Schematic of the working circuits [1]

In Table 1, Z and Y are the distributed series impedance and shunt admittance of the transmission line, respectively. μ , σ , and ϵ are the electrical constants of magnetic permeability, electrical conductivity, and dielectric constant of the electromagnetic shield, respectively.

A. Single-layer shielding

As shown in Fig.5(a), when an electromagnetic wave comes to the interface of two materials with different characteristic impedance, reflection occurs. Because the charging platform is a low impedance electromagnetic source, only the magnetic wave is considered [3]. The transmitted and reflected fields could be expressed as:

$$H_t = H_i \rho_t \quad (1)$$

$$H_r = H_i \rho_r \quad (2)$$

where ρ_t and ρ_r are the transmission and reflection coefficient respectively, and have the forms as shown in (3) and (4).

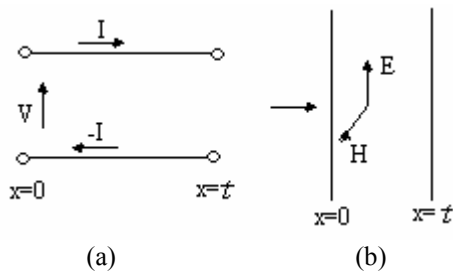


Fig. 4: Analogy of (a) transmission line and (b) electromagnetic shield [3]

TABLE I
COMPARISON OF THE TRANSMISSION LINE AND THE ELECTROMAGNETIC SHIELD

	Transmission line	Electromagnetic shield
Basic equations	$\frac{dV}{dx} = -ZI$ $\frac{dI}{dx} = -YV$	$\frac{dE}{dx} = -j\omega\mu H$ $\frac{dH}{dx} = -(\sigma + j\omega\epsilon)E$
Characteristic impedance	$Z_c = \sqrt{\frac{Z}{Y}}$	$\eta = \sqrt{\frac{j\omega\mu}{\sigma + j\omega\epsilon}}$
Propagation constant	$\Gamma = \sqrt{ZY}$	$\gamma = \sqrt{j\omega\mu(\sigma + j\omega\epsilon)}$

$$\rho_t = \frac{2\eta_a}{\eta_a + \eta_b} \quad (3)$$

$$\rho_r = \frac{\eta_b - \eta_a}{\eta_a + \eta_b} \quad (4)$$

When a single-layer shield is considered, there are two boundaries, as shown in Fig.5(b). At the first boundary, the source wave H_i is reflected and the transmitted field can be calculated out by (5) which has a similar form as in (1).

$$H_{t1}^1 = H_i \rho_t^1 \quad (5)$$

The transmission coefficient ρ_t^1 comes from the result of (3).

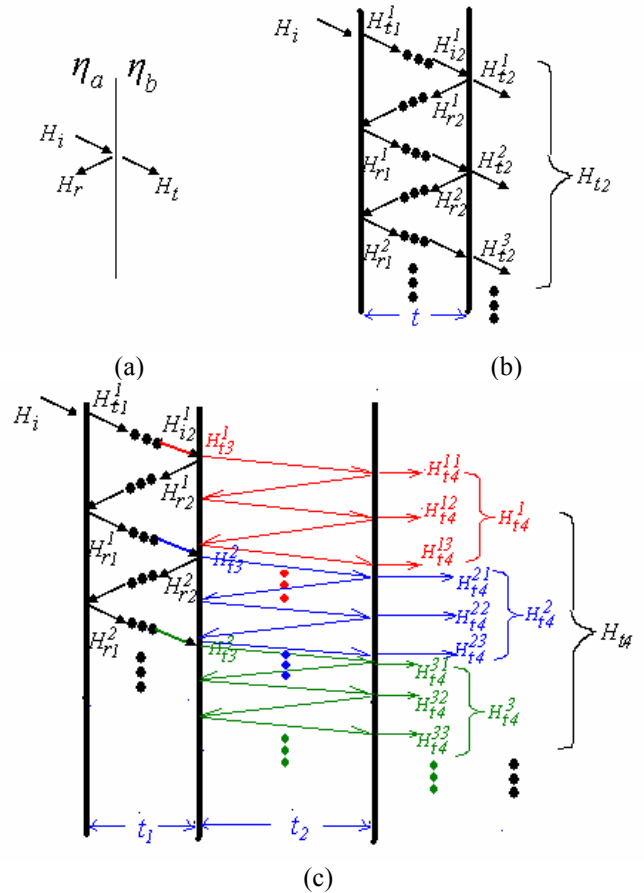


Fig. 5: Propagation of waves: (a) Single interface. (b) Single-layer shield. (c) double-layer shield

At this time, η_b denotes the characteristic impedance of the shield that can be calculated out from the equation in Table 1, and η_a denotes the incident wave impedance Z_w . From the discussion in [7], the incident wave impedance Z_w is equal to $j\mu\omega d/3$ (where d is the distance from the source to the measurement point as shown in Fig. 6) so as to meet the basic law of physics: reciprocity.

When the transmitted wave H_{t1}^1 goes through the shielding material, from the first boundary to the second boundary, the magnetic field is attenuated due to the absorption loss inside the barrier, and the attenuated wave could be expressed as:

$$H_{t2}^1 = H_{t1}^1 e^{-\gamma t} \quad (6)$$

where γ is the propagation constant that is listed in Table 1 and t is the thickness of the layer.

At the second boundary, another reflection occurs. The reflected and transmitted field H_{r2}^1 and H_{t2}^1 could be calculated as:

$$H_{r2}^1 = H_{t1}^1 e^{-\gamma t} \rho_r^2 = H_i \rho_t^1 e^{-\gamma t} \rho_r^2 \quad (7)$$

$$H_{t2}^1 = H_{t1}^1 e^{-\gamma t} \rho_t^2 = H_i \rho_t^1 e^{-\gamma t} \rho_t^2 \quad (8)$$

In calculating ρ_r^2 and ρ_t^2 from (3) and (4), it should be noticed here that η_a is the characteristic impedance of the shield, while η_b equals to the incident wave impedance Z_w .

Furthermore, infinite re-reflections occur inside the shield, as shown in Fig.5(b). And total field out of the shield is the sum of all the out-transmitted waves, which means:

$$H_{t2} = H_{t2}^1 + H_{t2}^2 + H_{t2}^3 + \dots = \frac{\rho_t^1 \rho_t^2 e^{-\gamma t}}{1 - \rho_r^1 \rho_r^2 e^{-2\gamma t}} H_i \quad (9)$$

The derivation of (9) could be found in the Appendix. The shielding effectiveness (SE) of one single-layer shield could be calculated with:

$$SE = \frac{H_{t2}}{H_i} = \frac{\rho_t^1 \rho_t^2 e^{-\gamma t}}{1 - \rho_r^1 \rho_r^2 e^{-2\gamma t}}$$

$$\rho_t^1 = \frac{2Z_w}{Z_w + \eta}$$

$$\rho_r^2 = \frac{2\eta}{Z_w + \eta} \quad (10)$$

$$\rho_r^1 = \frac{\eta - Z_w}{\eta + Z_w}$$

$$\rho_r^2 = \frac{\eta - Z_w}{\eta + Z_w}$$

where η and γ are the characteristic impedance and the propagation constant of the single-layer shield respectively, and t is its thickness.

B. Double-layer shielding

The double-layer shield could be analyzed with a similar method presented previously. The transmitted magnetic field from the first layer to the second layer is labeled as H_{t3} , as

shown in Fig.5(c). It consists of $H_{t3}^1, H_{t3}^2, H_{t3}^3, \dots$, which are similar with H_{t2}^n ($n=1,2,3,\dots$) in Fig.5(b) and could be expressed as:

$$H_{t3}^1 = H_i \rho_t^1 \rho_t^2 e^{-\gamma_1 t_1}$$

$$H_{t3}^2 = H_i \rho_t^1 \rho_t^2 e^{-\gamma_1 t_1} \rho_r^1 \rho_r^2 e^{-2\gamma_1 t_1} \quad (11)$$

$$H_{t3}^3 = H_i \rho_t^1 \rho_t^2 e^{-\gamma_1 t_1} (\rho_r^1 \rho_r^2 e^{-2\gamma_1 t_1})^2$$

$$\vdots$$

When H_{t3}^n ($n=1,2,3,\dots$) comes to the out-boundary of the second layer, multi-reflection also occurs. The out-transmitted field consists of $H_{t4}^n, H_{t4}^{n2}, H_{t4}^{n3}, \dots$, and could be expressed as:

$$H_{t4}^{n1} = H_{t3}^n \rho_t^4 e^{-\gamma_2 t_2}$$

$$H_{t4}^{n2} = H_{t3}^n \rho_t^4 e^{-\gamma_2 t_2} \rho_r^3 \rho_r^4 e^{-2\gamma_2 t_2} \quad (12)$$

$$H_{t4}^{n3} = H_{t3}^n \rho_t^4 e^{-\gamma_2 t_2} (\rho_r^3 \rho_r^4 e^{-2\gamma_2 t_2})^2$$

$$\vdots$$

The total field out of the second layer is the sum of the out-transmitted field:

$$H_{t4} = \sum_{n=1}^{+\infty} (H_{t4}^{n1} + H_{t4}^{n2} + H_{t4}^{n3} + \dots) \quad (13)$$

$$= \sum_{n=1}^{+\infty} \frac{H_{t3}^n \rho_t^4 e^{-\gamma_2 t_2}}{1 - \rho_r^3 \rho_r^4 e^{-2\gamma_2 t_2}}$$

$$= \frac{H_i \rho_t^1 \rho_t^2 \rho_t^4 e^{-\gamma_2 t_2} e^{-\gamma_1 t_1}}{(1 - \rho_r^3 \rho_r^4 e^{-2\gamma_2 t_2})(1 - \rho_r^1 \rho_r^2 e^{-2\gamma_1 t_1})}$$

So the shielding effectiveness of double-layer shield could be calculated with:

$$SE = \frac{H_{t4}}{H_i} = \frac{\rho_t^1 \rho_t^2 \rho_t^4 e^{-\gamma_2 t_2} e^{-\gamma_1 t_1}}{(1 - \rho_r^3 \rho_r^4 e^{-2\gamma_2 t_2})(1 - \rho_r^1 \rho_r^2 e^{-2\gamma_1 t_1})}$$

$$\rho_t^1 = \frac{2Z_w}{Z_w + \eta_1}$$

$$\rho_r^2 = \frac{2\eta_1}{\eta_1 + \eta_2}$$

$$\rho_t^4 = \frac{2\eta_2}{\eta_2 + Z_w}$$

$$\rho_r^1 = \frac{\eta_1 - Z_w}{\eta_1 + Z_w}$$

$$\rho_r^2 = \frac{\eta_1 - \eta_2}{\eta_1 + \eta_2} \quad (14)$$

$$\rho_r^3 = \frac{\eta_2 - \eta_1}{\eta_1 + \eta_2}$$

$$\rho_r^4 = \frac{\eta_2 - Z_w}{\eta_2 + Z_w}$$

where η_1 and η_2 are the characteristic impedance of the two

layers, while t_1 and t_2 are their thickness respectively.

By using (10) and (14), the shielding effectiveness (SE) of the single ferrite plate, the single copper sheet and the double-layer shield could be calculated respectively and the results are plotted as solid lines in Fig.8. In the calculation, relative permeability, μ_r of the 4F1 ferrite material is kept as a constant of 80. The distance from the source to the measurement point, d is the same with that in experiment and is equal to 5 mm.

IV. MEASUREMENT

In the experiment, the charging platform is simplified as a coreless PCB transformer [9]. As shown in Fig.6, a transmitting and a receiving coreless PCB windings are placed at a specified distance on either side of the shield and measurements are taken with and without the shield to evaluate the SE [7][8]. The distance between these two windings is 5mm. The geometric parameters of these two windings and the shield are listed in Table 2. A RF Power Amplifier is used to drive the transmitting winding at different frequencies through a 1Ω measurement resistor. The current in the transmitting winding is kept at 0.5 A (RMS). The receiving winding is open-circuit and the voltage across it is measured. For example, Fig.7 gives out the experimental results when the frequency is 200 kHz, which is within the range of the working frequency of the charging platform. In Fig.7, *Ch1* is the voltage across the 1Ω measurement resistor and is kept around 0.5 V, and *Ch2* is the voltage across the receiving winding. Fig.7(a)-(d) show the situations (a) without shielding, (b) with 4F1 ferrite plate as a single-layer shield, (c) with copper sheet as a single-layer shield and (d) with 4F1 ferrite plate plus copper sheet as a double-layer shield respectively. It must be noticed that the scales of *Ch2* in Fig.7(a)-(d) are 100 mV/div, 10 mV/div, 10 mV/div and 1 mV/div respectively. From the measurement results, the SE of such three situations at 200 kHz could be determined:

$$SE_{4F1} = 20 \log_{10}(175/10.7) = 24.3dB$$

$$SE_{copper} = 20 \log_{10}(175/21.5) = 18.2dB$$

$$SE_{double} = 20 \log_{10}(175/0.76) = 47.2dB$$

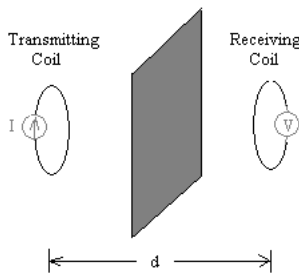
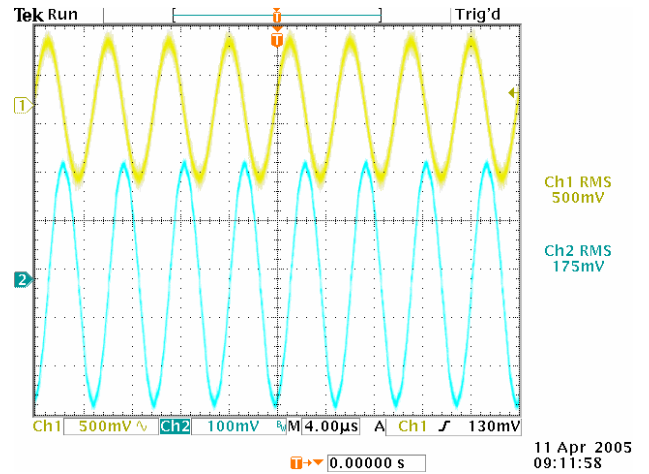
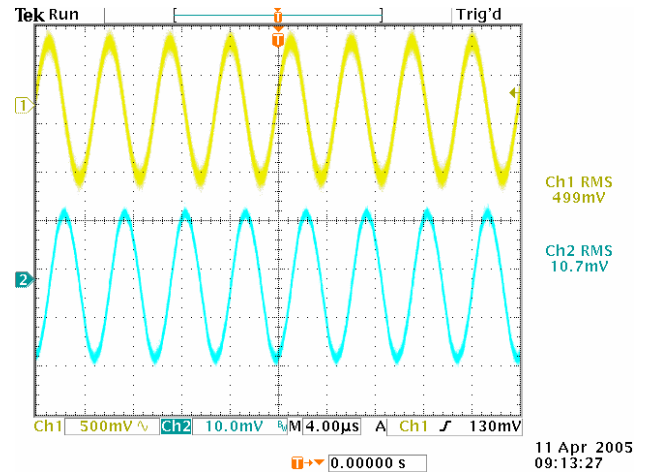


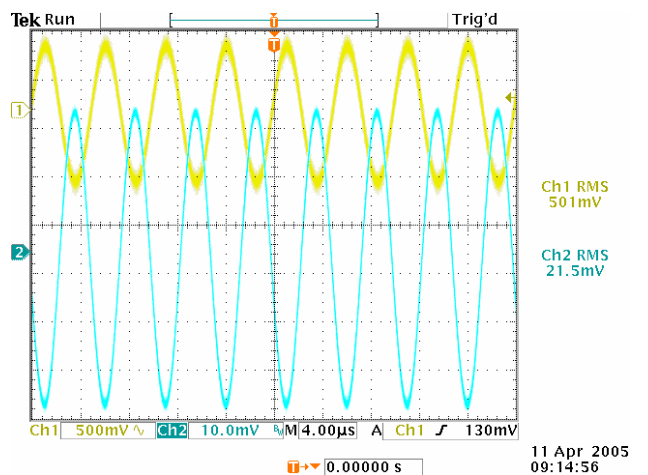
Fig. 6: Structure of the measuring sets



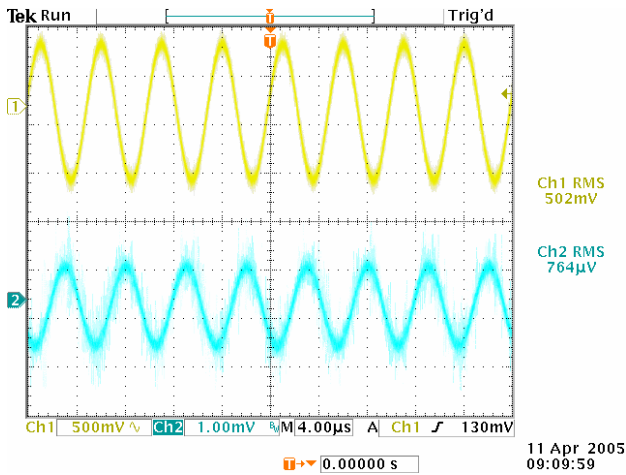
(a): Without shielding (upper trace: 0.5A/div.; bottom trace: 100mV/div)



(b): With 4F1 ferrite plate as shield (upper trace: 0.5A/div.; bottom trace: 10mV/div)



(c): With copper sheet as shield (upper trace: 0.5A/div.; bottom trace: 10mV/div)



(d): With a double-layer shield (upper trace: 0.5A/div.; bottom trace: 1mV/div)

Fig. 7: Measured voltages at the frequency of 200 kHz

The measured voltages at other frequencies are listed in Table 3 and the shielding effectiveness in dB is summarized by the dots in Fig.8. From the calculated and measured results in Fig.8, it could be seen that:

- the thin 4F1 ferrite has almost the same SE over the frequency range from 10 kHz to 3 MHz, but its SE value of around 20 dB is not enough in many applications;
- the SE of a thin copper shield rises greatly with the increase of frequency, which means that copper can be a good shielding material when the frequency is high enough (as long as the copper loss is acceptable);
- in the working frequency range of the charging platform (from 100 kHz to 500 kHz), this double-layer shield shows a good shielding effectiveness, entirely above 40 dB.

TABLE II
GEOMETRIC PARAMETERS OF THE MEASURING SET

Geometric Parameter	Transmitting winding	Receiving winding
Copper Track Width	0.4 mm	0.1 mm
Copper Track Thickness	140 μm	140 μm
Number of Turns	10	10
Winding Radius	12 mm	12 mm
Dimensions of Ferrite Plate	63mm × 63mm × 0.4mm	
Dimensions of Copper sheet	63mm × 63mm × 0.07mm	

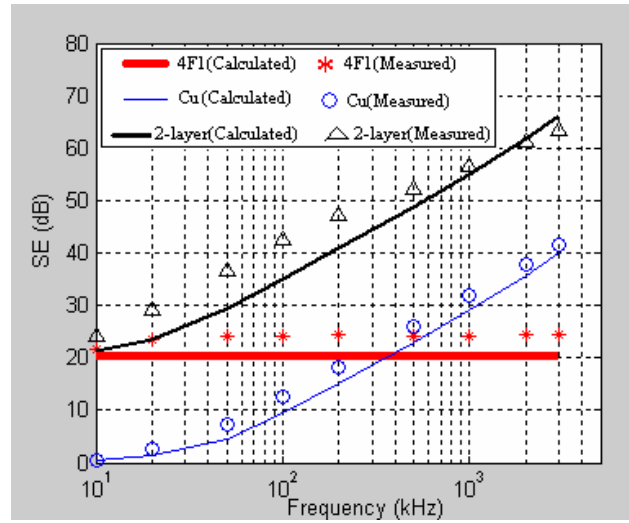


Fig. 8: Calculated and measured Shielding Effectiveness in dB

TABLE III
MEASURED RESULTS

Frequency(kHz)	Measured Voltage (mV)			
	No shield	Ferrite	Copper	2-layer
10	8.93	0.75	8.60	0.56
20	18.1	1.23	13.1	0.61
50	44.5	2.81	19.0	0.65
100	89.3	5.48	21.2	0.68
200	175	10.7	21.5	0.76
500	432	26.7	21.7	1.08
1000	840	52.0	21.7	1.25
2000	1660	100	21.0	1.43
3000	2510	150	20.6	1.68

V. CONCLUSION AND DISCUSSION

This paper presents a theoretical analysis and practical evaluation of a double-layer EM shielding structure. This analysis is based on the extended transmission line theory and can generate fast and reasonably accurate solutions without using the time-consuming finite-element methods. Both calculated and measured results agree well and have confirmed the good shielding effectiveness of this double-layer structure (>40dB) in the working frequency range from 100 kHz to 500 kHz of the planar battery charging platform.

For applications with shielding requirement at a lower frequency (e.g. <100 kHz), the shielding effectiveness of the double-layer shield in this example may not be high enough. The main reason for this is that, at low frequency, only the ferrite plate acts as the main contribution of the shielding and copper sheet is not effective as a shield. The material chosen (4F1) has a relatively low permeability ($\mu_r=80$) compared with other ferrite materials like 3C91 ($\mu_r=3000$). With the equations presented in this paper, it could be predicted that such ferrite material (3C91) could achieve a high SE up to 60 dB due to its high permeability at low frequency. But the permeability and SE of such material decreases rapidly with

the increase of frequency [11], while the SE of copper increases with frequency. So with the help of copper sheet, the double-layer structure with other ferrite material (like 3C91) may exhibit a wide-band shielding effectiveness. Such practical work could be carried out in the future with the help of the analysis presented in this paper.

APPENDIX

Referred to Fig.5(b), the derivation of (9) is:

$$\begin{aligned}
 H_{t1}^1 &= H_i \rho_t^1 \\
 H_{t2}^1 &= H_{t1}^1 e^{-\gamma} \rho_t^2 = H_i \rho_t^1 e^{-\gamma} \rho_t^2 \\
 H_{r2}^1 &= H_{t1}^1 e^{-\gamma} \rho_r^2 = H_i \rho_t^1 e^{-\gamma} \rho_r^2 \\
 H_{r1}^1 &= H_{r2}^1 e^{-\gamma} \rho_r^1 = H_i \rho_t^1 e^{-2\gamma} \rho_r^1 \rho_r^2 \\
 H_{t2}^2 &= H_{r1}^1 e^{-\gamma} \rho_t^2 = H_i \rho_t^1 e^{-3\gamma} \rho_r^2 \rho_r^1 \rho_t^2 \\
 H_{r2}^2 &= H_{r1}^1 e^{-\gamma} \rho_r^2 = H_i \rho_t^1 e^{-3\gamma} (\rho_r^2)^2 \rho_r^1 \\
 H_{r1}^2 &= H_{r2}^2 e^{-\gamma} \rho_r^1 = H_i \rho_t^1 e^{-4\gamma} (\rho_r^2 \rho_r^1)^2 \\
 H_{t2}^3 &= H_{r1}^2 e^{-\gamma} \rho_t^2 = H_i \rho_t^1 \rho_t^2 e^{-5\gamma} (\rho_r^1 \rho_r^2)^2 \\
 &\dots \\
 H_{t2} &= H_{t2}^1 + H_{t2}^2 + H_{t2}^3 + \dots \\
 &= H_i \rho_t^1 \rho_t^2 e^{-\gamma} (1 + e^{-2\gamma} \rho_r^1 \rho_r^2 + (e^{-2\gamma} \rho_r^1 \rho_r^2)^2 + \dots) \\
 &= \frac{\rho_t^1 \rho_t^2 e^{-\gamma}}{1 - \rho_r^1 \rho_r^2 e^{-2\gamma}} H_i
 \end{aligned}$$

ACKNOWLEDGMENT

The authors would like to thank the Research Grant Council of Hong Kong for its support for this project (RGC

Reference No.: CityU 1223/03E). Mr. X. Liu is grateful to the City University of Hong Kong for providing the research scholarship and studentship for his Ph.D study.

REFERENCES

- [1] S.Y.R.Hui and W.C.Ho, "A new generation of universal contactless battery charging platform for portable consumer electronic equipment", *PESC. 35th Power Electronics Specialists Conference*, pp. 638-644, Jun. 2004.
- [2] S.C. Tang, S.Y.R.Hui, H.S.-H. Chung, "Evaluation of the shielding effects on printed-circuit-board transformers using ferrite plates and copper sheets", *IEEE Trans. Power Electron*, vol. 17, pp.1080 – 1088, Nov. 2002.
- [3] R. B. Schulz, V.C.Plantz, D.R.Brush, "Shielding Theory and Practice", *IEEE Trans. on Electromagnetic Compatibility*, vol. 30, pp. 187-201, Aug. 1988.
- [4] S.A.Schelkunoff, *Electromagnetic Waves*. Princeton, NJ: D.Van Nostrand, 1943.
- [5] "Material specification: 4F1", Soft Ferrites and Accessories CDROM, Ferroxcube, 2005.
- [6] D.A.Weston, *Electromagnetic Compatibility: principles and applications*, NY: Marcek Dekker, 1991.
- [7] J. R. Moser, "Low-Frequency Low Impedance Electromagnetic Shielding", *IEEE Trans. on Electromagnetic Compatibility*, vol. 30, pp. 202-210, Aug. 1988.
- [8] Y. Trenkler, L. E. McBride, "Shielding Improvement by multi-layer Design", *1990 IEEE International Symposium on Electromagnetic Compatibility*, pp. 1-4, 21-23 Aug. 1990.
- [9] Hui S.Y.R. and Tang S.C., 'Coreless Printed-circuit board (PCB) transformers and operating techniques' US patent application serial number 09/316735
- [10] Hui S.Y.R. and Tang S.C., "Planar printed circuit-board transformers with effective electromagnetic interference (EMI) shielding", US patent 09/883,145 2003
- [11] "Material specification: 3C91", Soft Ferrites and Accessories CDROM, Ferroxcube, 2005
- [12] Hui S.Y.R., "Planar inductive battery charger", UK patent application (GB2389720) and PCT patent application.
- [13] Hui S.Y.R., "Battery charging system", Patent application number GB 2399446
- [14] Hui S.Y.R., "Apparatus for energy transfer by induction", Patent application number GB2389767